Colloids and Surfaces B: Biointerfaces 204 (2021) 111810

Contents lists available at ScienceDirect

Colloids and Surfaces B: Biointerfaces

journal homepage: www.elsevier.com/locate/colsurfb

Breast adenocarcinoma-derived exosomes lower first-contact de-adhesion strength of adenocarcinoma cells to brain endothelial layer

Csilla Fazakas [a], Mihály Kozma [a,b], Kinga Molnár [a,b], András Kincses [a], András Dér [a], Adrienn Fejér [c], Barnabás Horváth [c], Imola Wilhelm [a,d], István A. Krizbai [a,d], Attila G. Végh [a,*]

[a] Institute of Biophysics, Biological Research Centre, Szeged, Hungary
[b] Theoretical Medicine Doctoral School, University of Szeged, Szeged, Hungary
[c] Faculty of Science and Informatics, University of Szeged, Szeged, Hungary
[d] Institute of Life Sciences, Vasile Goldiş Western University, Arad, Romania

ARTICLE INFO

Keywords:
Atomic force microscope
Single-cell force spectroscopy
Metastasis
Breast cancer
Exosomes

ABSTRACT

Despite of advances in modern therapeutics, one of the most feared complications of cancer are brain metastases, which often cause life impairing profound neurological symptoms and premature death. Breast adenocarcinoma is among the leading "sources" of brain metastases. Since the central nervous system lacks a classical lymphatic circulation, invading metastatic cells can reach the brain parenchyma only through haematogenous routes and must breach the blood-brain barrier (BBB). The key step before the transmigration of metastatic cells through the highly regulated interface of the BBB is the establishment of firm adhesion between the tumor cell and the cerebral endothelial layer. Using atomic force microscopy, as a high resolution force spectrograph, direct measurements of intercellular interactions was performed between living adenocarcinoma cells and a confluent endothelial layer pre-treated with carcinoma cell-derived exosomes. By immobilization of a living adenocarcinoma cell to an atomic force microscope's cantilever, intercellular de-adhesions were directly measured by single cell force spectroscopy (SCFS) at quasi-physiological conditions. De-adhesion dynamics and strength was characterized by several different calculated parameters, involving aspects of both membrane and cell surface related factors. Our results indicate that de-adhesion strength was lower in case of exosome pre-treated endothelial cells as compared to non-treated controls. Breast adenocarcinoma-derived exosomes have direct effect on de-adhesion pattern of brain endothelium.

1. Introduction

The most common brain malignancies are not locally developed but due to metastases, presenting the most frequent neurological complications of systemic cancer and result in poor prognosis for patients [1]. Although incidence of brain metastases might be underestimated, breast cancers are in the second place regarding the origin of metastatic brain lesions [2].

Several factors play important role in metastatic site selection, among which role of tumor cell derived exosomes and micro-vesicles gained visibility only recently [3]. These small membrane-encapsulated vesicles may play important roles in several aspects of metastatic processes [4,5]. Their large variety, regarding both size and content makes it extremely difficult to address and answer simple but important questions related to their function. As the diameter of exosomes is, by definition, below the optical limit, tools for morphological investigations are limited. Although some emerging super-resolution techniques could enlarge our knowledge in the near future, atomic force microscopy (AFM) is straightforward and versatile technique in the field of exosome characterization.

Atomic force microscopy has evolved to a powerful high-resolution imaging and force sensing tool in biology and medicine [6], where cancer biology and metastatic processes are not exceptions [7]. As the AFM can operate in liquid environment and act as a picoNewton range force sensor, offers enlarging potential in the investigation of extracellular vesicles and exosomes [8,9]. Extracellular vesicles, as a fraction of sub cellular vesicles have their diameter from few tens up to few hundreds of nanometer which makes them ideal candidate for AFM-based investigations.

Adhesion molecules on the surface of tumor cell-derived exosomes

* Corresponding author at: BRC Szeged, Temesvári krt 62, Szeged, H-6726, Hungary.
E-mail address: vegh.attilagergely@brc.hu (A.G. Végh).

https://doi.org/10.1016/j.colsurfb.2021.111810
Received 17 December 2020; Received in revised form 31 March 2021; Accepted 28 April 2021
Available online 30 April 2021

may have important role in organotropic metastasis [10]. Tumor cell-derived exosomes might influence biophysical properties of source cells as showed in case of hepatocellular cancer cells [11]. Exposure to tumor derived micro-vesicles has effect on roughness and morphology of gastric adenocarcinoma cells [12]. Exosomes can have different nano-mechanical properties depending on malignancy, influence endothelial leakiness and might be implicated in monolayer disruption [13]. Exosomes and micro-vesicles may influence biophysical properties of both tumor and target cells which might be crucial for metastasis progression [14].

As the brain lacks classical lymphatic circulation, invading tumor cells must breach the tight layer of brain endothelium in order to establish colonies in the parenchyma. Although this multistep process has several pitfalls and metastasis is not counted as an effective process, the first and crucial step is for tumor cells to establish a firm connection to the endothelial cells. Strength of this linkage may be different when endothelial cells are pre-exposed to tumor-derived exosomes. Classical cell-adhesion assays do not provide direct information on dynamics of intercellular linkage formation.

Exosomes are key mediators of pre-metastatic niche formation. They transport bioactive molecules to distant metastatic sites to reprogram recipient cells. As a result, tumor cells prepare the receiving organs to be more permissive to metastatic outgrowth [3,15,16]. By forming the first defense line of metastatic organs against invading tumor cells, endothelial cells are the first targets of tumor exosomal remodeling. However, it is largely unknown how exosomes influence transendothelial migration of tumor cells.

The aim of the present study was to investigate whether pre-treatment of brain endothelial cells with tumor derived exosomes does have any influence on the de-adhesion and un-binding dynamics between tumor and endothelial cells. This step might be crucial in the successful brain colonization and its detailed understanding may contribute to successful prevention. Up to our best knowledge, direct cell de-adhesion measurements targeting the effect of tumor-derived exosomes on de-adhesion strength of tumor cells from brain endothelial cells were not yet reported. Hereby, effect of triple negative breast adenocarcinoma derived exosomes on de-adhesion strength of host tumor cells to brain endothelial layer is presented. The used setup eliminates most of the probing cell-introduced uncertainty by measuring the de-adhesion pattern of the very same tumor cell to differently treated layers of brain endothelium. Furthermore, we use the direct and high resolution method based on single cell force spectroscopy to characterize the dynamics of de-adhesion pattern of intercellular linkage.

2. Materials and methods

2.1. Cell culture

The hCMEC/D3 human microvascular cerebral endothelial cells (shortly D3, [17]) were grown on rat tail collagen-coated dishes in EBM-2 medium (Lonza) supplemented with EGM-2 Bullet Kit (Lonza) and 2.5 % FBS (Sigma-Aldrich). MDA-MB-231 human breast cancer cells were kept in DMEM medium (Sigma-Aldrich) supplemented with 5% FBS (Lonza). Before measurements, all adenocarcinoma cells were labeled with CellTracker™ Red CMTPX Dye (Life Technologies) following the manufacturer's instructions.

4 well micro-insert chambers (Ibidi, Cat. No. 80466) were used to compartmentalize the D3 cells cultured in parallel in order to reduce passage and handling related variance. One compartment was always kept for non-treated cells, while the cells cultured in two other well-pairs received MDA-derived exosomes in different concentration (2.5, 5, 10, 20 μg/mL; pairing 2.5 with 10 and 5 with 20) for 24 h prior to experiments. During measurements, the silicon insert was removed from the surface of the Petri dish. Cells were washed and given serum free L-15 Leibovitz Medium (Sigma-Aldrich).

2.2. MDA cells-derived exosome harvesting

MDA-MB-231 cells were cultured in exosome-depleted 2 % FBS containing media in 10 cm diameter dishes until 80 % confluence. Cells were given fresh media and kept for additional 24 h prior to exosome harvesting. In order to obtain intact exosomes, they were isolated by differential centrifugation method: 700 x g, 5 min, 1000 x g, 8 min, 10,000 x g, 30 min (microvesicles), the supernatant was filtered through a 0.22 μm pore size membrane (Millipore) followed by centrifugation at 150,000 x g, 90 min all at 4 °C. Exosomes were collected in PBS and stored at -20 °C. Exosome concentration was measured by their protein content using micro-bicinchoninic acid method (MicroBCA, Thermo Fisher Scientific).

2.3. PKH26-staining protocol for MDA exosomes uptake

MDA-MB-231 derived exosomes were labeled with fluorescent dye PKH26 using the PKH26 labeling kit (Sigma-Aldrich). Briefly 1,5 mg/mL of exosomes in PBS were mixed with 2 μL of PHK26 dye (1:500) diluted in diluent C (1 : 1 v/v) for 5 min. The labelling was stopped by adding 1% BSA in PBS to the mixture and centrifuged at 150,000 x g for 90 min to pellet the PKH26 labeled exosomes. The exosome pellet was further washed once with PBS by ultracentrifugation at 150,000 x g for 90 min, to remove any free dye. Finally, the exosome pellet was resuspended in 200 μL PBS, protein concentration was determined again as previously described, labelled exosomes were used for uptake studies.

PKH26 labeled MDA-derived exosomes were placed onto confluent hCMEC/D3 cells grown on glass coverslips in 10 ug/mL and 20 ug/mL concentrations in 5 parallels in serum-free EBM-2 medium. Separately 5 samples were given PKH26 ultracentrifuged the same way as the exosomes, as dye control. After 24 h incubation, endothelial cells were extensively washed with PBS and fixed with 3% PFA for 10 min, followed by nuclei staining with Hoechst 33342 (1 ug/mL, Sigma-Aldrich). The coverslips were mounted with Fluoromount G (Thermo Fisher Scientific) anti-fading mounting medium. Samples were analyzed with Leica SP5 confocal microscope (Leica Biosystems) using 63x objective.

2.4. Western blot analysis

Exosomes were lysed in ice-cold lysis buffer (20 mMTris, 150 mMNaCl, 0.5 % Triton X-100, 1% sodium deoxycholate, 0.1 % sodium dodecyl sulphate, 1 mM sodium vanadate, 10 mMNaF, 1 mM EDTA, 1 mMPefabloc®), incubated on ice for 30 min followed by centrifugation at 10,000 *g* for 10 min at 4 °C. Laemmli buffer was added to samples and incubated at 95 °C for 3 min. Proteins were electrophoresed with standard denaturing SDS-PAGE procedures and blotted on PVDF (0.2 μm pore size, BioRAD) membranes. Blocking the nonspecific binding capacity of the membranes was carried out at room temperature for 30 min in TBS-T (Tris buffered saline with 0.1 % Tween-20) containing 3% BSA. Membranes were incubated with primary antibodies against Grp94 (Cell Signaling), Hsp70 (BD Biosciences), Alix (Santa Cruz) overnight at 4 °C in TBS-T. After washing the membranes three times for 5 min in TBS-T, the blots were incubated with the secondary antibodies diluted in TBS-T, then washed again three times for 10 min in TBS-T. Immunoreaction was visualized with Clarity Chemiluminescence Substrate (Bio-Rad) in a ChemiDoc MP System (Bio-Rad).

2.5. Dynamic light scattering

The size distribution of the samples was determined using dynamic light scattering (DLS, Zetasizer Nano ZS, Malvern instruments). The device is equipped with a He-Ne laser with the wavelength of 633 nm. The method is based on the scattering intensity fluctuation over time due to the Brownian motion of the small particles in the suspension. Autocorrelation function is used to calculate the size distribution from the recorded intensity trace. The resulting size values are equal to the

hydrodynamic radius of spheres based on the Stokes–Einstein equation. Since the determined size is the diameter of a sphere that moves as the scattering object, the method accurately measures the size of the exosomes. All measurements were carried out in PBS, at room temperature (25 °C), performing minimum 3 measurements for each sample (between 11–16 runs each) with the automatic resolution and parameters calculated by the driver software of the instrument.

2.6. Atomic force microscope

Experiments were carried out with an Asylum Research MFP-3D atomic force microscope (Asylum Research, Santa Barbara, CA; driving software IgorPro 6.32A, Wavemetrics), mounted on a Zeiss Axiovert 200 optical microscope.

For imaging, overall gold-coated silicon nitride cantilevers, holding a v-shaped tip with 30 nm radius of curvature (BL RC150VB-A by Olympus) were used. The cantilevers had a nominal spring constant of 50 pN/nm and resonant frequency of 37 kHz. Images were recorded in PBS after immobilization of MDA cell- derived exosomes onto a glass surface. Presuming that the surface of exosomes contains proteins, a glutaraldehyde based immobilization method used for proteins was used [18].

The de-adhesion experiments were performed with gold-coated n-type silicon rectangular tipless cantilevers, nominal resonant frequency 14 kHz, spring constant of 50 pN/nm (MikroMasch, Tallinn, Estonia). Each probe was calibrated prior to experiment, based on two well-established spring constant calibration techniques, the thermal noise method [19,20] and the Sader method [21,22].

2.7. Force measurements

Freshly cultured MDA cell was immobilized at the very end of a tipless cantilever with the help of ConcanavalinA mediated linkage [23]. During a force measurement cycle, the tumor cell was brought into contact with surface adhered endothelial cell. Each cycle consisted of lowering and pulling back the cell decorated cantilever until the pre-set deflection was reached as depicted on panel A of Fig. 1.

Force curves were recorded at constant loading speed (2 μm/s) and sampling frequency (0.5 kHz). Total force distance was kept at 8 μm with maximum load of 2 nN. For each force measurement, between the maximum load and start of retrace a dwell time of 3 s was applied [24]. This waiting time was set based on our previous experience to be sufficient for building up intercellular bonds. Curves with partial detachment were excluded from data analysis. Treated and control cells were measured in randomized order to exclude sequential errors. Furthermore, only those experiments were taken into calculation when the randomly effectuated sequence gave twice the same result.

2.8. Data analysis

A custom-made MATLAB routine was used to extract the above mentioned parameters. Briefly, adhesion work was calculated as the area under the curve colored green (dark + light green) on panel B of Fig. 1. Values of Adhesion Force were considered as the difference between the maximal downward deflection of the cantilever compared to the initial non-contact level. Individual rupture events were identified as higher differences as three fold the standard deviation of the last 50 points of each respective force curve. Rupture size was calculated as the level differences at the identified rupture events. Such places on retraction phases of a typical force curve are marked with pink squares on panel B Fig. 1, magnified at same figure's inset.

Presented data comes from ten in case of exosome treatment and seven parallels in case of control experiments. All histograms shown represent a probability distribution of the respective parameter, since for proper comparison all were divided with the number of data elements considered. Each obtained histogram was fitted with a bell curve, as represented on Fig. 5.

3. Results

The goal of our experiments was to compare the de-adhesion forces of breast adenocarcinoma cells from human brain endothelial layer in presence or absence of carcinoma cell-derived exosomes.

Exosomes were characterized based on widely used marker proteins Alix, Hsp70 and absence of the endoplasmic reticulum chaperone molecule Grp94 (panel A of Fig. 2).

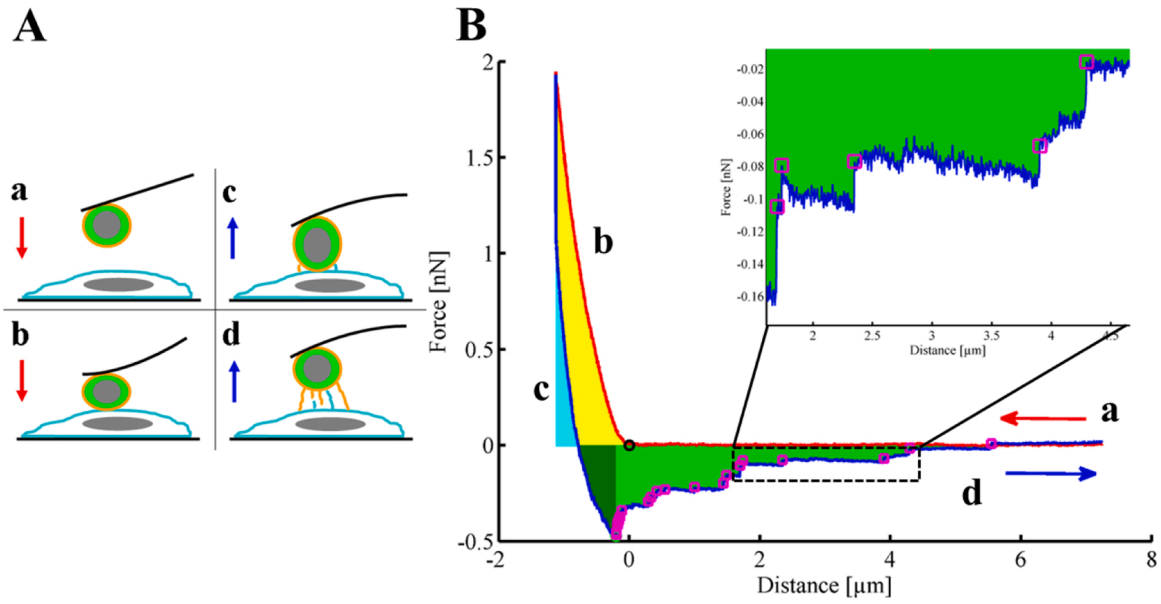

Fig. 1. Panel A: Schematic representation of a force cycle between a tumor cell immobilized at the very end of a tipless cantilever and surface adherent endothelial cell: lowering (a), pushing phase (b), early retracting (c), detachment (d). Panel B: Typical Force-Distance curve recorded between tumor and endothelial cell. Lowering is marked with red and retraction with blue, letters from a to d represent the phases depicted in panel A. Contact point is marked with "o", while places of stairs like rupture events with pink squares. Specific parameters are highlighted with colored areas as follows: Pull-off force, adhesion work (light + dark green). Inset: magnified portion of retrace with individual de-adhesion events highlighted.

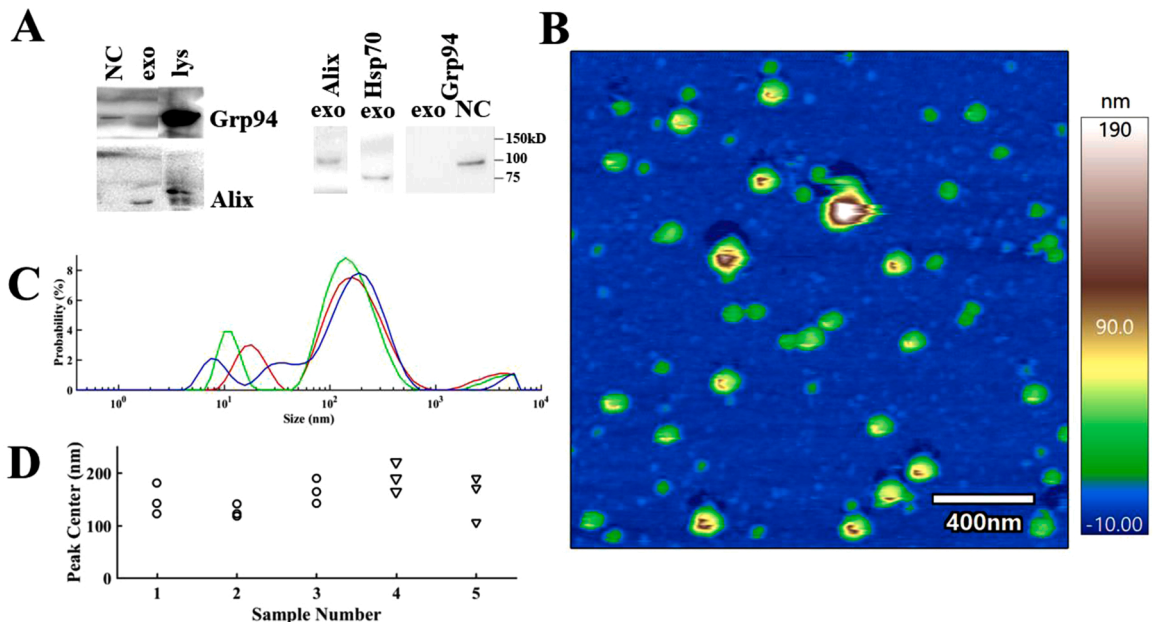

Fig. 2. Panel A: Characterization of MDA-MB-231 cells-derived exosomes based on the absence of Grp94 and on the positive expression of Alix and Hsp70 proteins. Representative western blots are shown of two parallel experiments. Micro vesicles served as negative control (NC). Lys stands for MDA cell lysate. Panel B: Height image of MDA-derived exosomes, immobilized onto glass surface. Image recorded in PBS. Panel C: Size (characterized by particle diameter) distribution of exosomes as measured by Dynamic Light Scattering. Representative data shows three consecutive measurement of the same sample of number 3 on panel D. Panel D: Overall comparison of highest peak positions (size of most abundant particles) from DLS measurements of the used samples.

Size distribution and morphology of exosomes was measured by dynamic light scattering and AFM. As it can be observed in panel B and C of Fig. 2, predominantly the vesicles with diameter from 100 to 200 nm were selected for experiments.

Size distribution and morphology by AFM has confirmed the presence of intact particles around 100–200 nanometer (see panel B of Fig. 2).

After characterization of the isolated exosomes, their uptake by endothelial cells was visualized. Presence of fluorescently stained exosomes around the nuclei of the endothelial cells is presented by Fig. 3. Non-bound or not uptaken exosomes were washed prior to imaging, therefore only those can be seen on the presented fluorescent images which were internalized by endothelial cells. Most of the exosomes accumulated around the nuclei, few of them were positioned in other cytoplasmic regions. As the orthogonal slices of the right panel shows, the exosomes are at the same height with the nuclei, which clearly underlines their intra-cellular position.

The simplest and most straightforward method to compare the established linkage between two living cells is to measure their de-adhesion force. Cells were brought together until a pre-defined load was exerted on them, succeeded by a short dwell time of 3 s, after which they are pulled apart. Schematic details of this process can be seen in panel A of Fig. 1. Detachment is showed by subpanels **c** and **d** of the aforementioned picture. The de-adhesion force between the two cells is the deflection opposite to load of the cell decorated cantilever, which is detailed in panel B of Fig. 1. Basically, the force needed to separate the two cells appears as the difference between the minimum and the end point of the blue section on the presented curve. Distribution of these values is presented in panel A of Fig. 4 with the help of box and whisker plots.

Slightly more complex parameter to characterize the intercellular linkage is the separation energy or de-adhesion work. This is extracted as the area under the retraction curve in blue in panel B of Fig. 1, taken between the two non-deflection states of the cantilever. This parameter is marked as (light and dark) green area on the aforementioned picture.

In both cases, the de-adhesion force and separation energy, a remarkable decrease can be observed if the endothelial layers were treated with exosomes (see panel B of Fig. 4).

The linkage strength can be further characterized by the number of rupture events observed during separation of the cells. These events can be counted as sudden level difference on the retraction part of the recorded signals. Such events are presented and highlighted on the inset of panel B of Fig. 1 by small magenta squares.

These events are fingerprints of the established quick intercellular connection. As panel C of Fig. 4 depicts, only slight inclination towards smaller numbers can be spotted in case of exosome treatment. Although the medians are practically similar in all cases, the larger values seem to occur less frequently.

Besides the number of recorded rupture events, their size carries important information about the types of formed intercellular connections. As shown at panel A of Fig. 5, larger values than 40 pN practically do not occur. However, in case of 10 μg/mL exosome treatment even these rupture sizes present a slight shift towards lower values.

Similar trend can be observed in case of where the detected ruptures occurred. Their distribution shows shift towards lower values as presented by panel B of Fig. 5.

By comparing at what pulling force the rupture occurred, our results indicate that in case of exosome treated endothelial cells these values are lower (see panel C of Fig. 5).

Due to the fact that in every experiment the de-adhesion strength of a single adenocarcinoma cell is tested to endothelial layers, which might show considerable differences, the overall comparison of parallel experiments is possible only by calculating the relative ratios to each nontreated case. Such a comparison can be found in the Fig. 6, which summarizes data from all the preformed experiments.

All pre-treated cases show lower values compared to non-treated ones. As the non-treated ones practically do not differ from each other any of them might be the one to compare at. By calculating all possible scenarios, we have found no differences between the control groups. Since they were measured in random order this underlines that they are practically indistinguishable. This excludes the chances that the probe cell exhibits different de-adhesion potential within the time of the experiment.

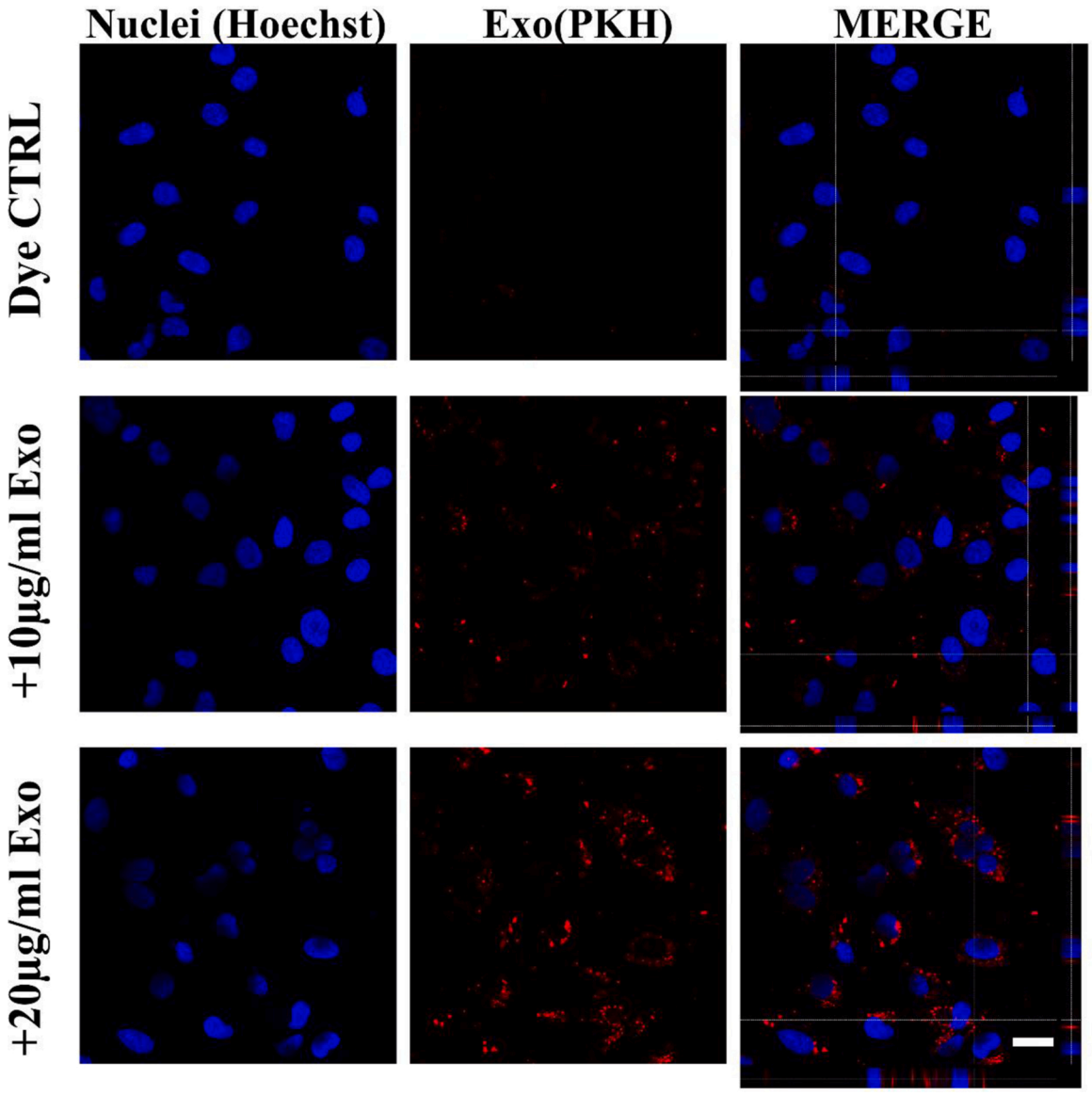

Fig. 3. Uptake of exosomes by endothelial cells after 24 h. Right panel shows orthogonal slices along the marked lines on the merged fluorescent images. Scale bar is 20 μm. All images were recorded at uniform magnification.

4. Discussion & summary

Tumor organotropism is one of the most difficult puzzle to solve regarding cancer development. Driving mechanisms and exact details which govern these processes are largely unexplored so far. Lately, attention has been turned towards tumor-derived exosomes, as potential targets for organ dependent therapies [5]. It is suggested that the presence of exosomes in future metastatic sites might enhance successful colonization [10]. It is worth to mention, that brain seeking tumor cell released exosomes appear to be more efficient in comparison to those originated from parental tumor cells [25]. Due to the complexity of the phenomena and lack or limited possibilities for real time and direct models majority of the results is hardly applicable outside their narrow field.

Breaching the blood-brain barrier is a necessary but not deterministic pre-requisite of brain colonization. As the brain lacks classical lymphatic circulation, hematogenous routes are of primordial importance. As a first step of this process blood-travelling tumor cells have to establish firm enough connections to brain endothelial cells, which is eventually followed by their transmigration to brain tissue.

Mechanistic factors and forces are crucial in the progress of metastasis, therefore deciphering their role might lead to unexpected results. Many independent factors can modulate the intercellular binding abilities, from the thickness of the glycocalyx to surface resident cell adhesion molecules [26,27].

Our aim was to keep the experimental setup as simple as possible. In the present study, de-adhesion strength of human breast adenocarcinoma cells from brain endothelial layer was tested upon pre-treating the endothelial cells with carcinoma cell-derived exosomes.

Size distribution of exosomes was measured by DLS and AFM images (Fig. 2). Exosomes were characterized based on the presence of widely used exosome marker Hsp70, the ESCRT (endosomal sorting complexes required for transport)-associated protein Alix and the absence of endoplasmic reticulum chaperone molecule Grp94 (panel A of Fig. 2). Our presumption was, that the pre-treatment with exosomes might alter the de-adhesion pattern of tumor cells brought in contact with endothelium. This scenario models first contact of blood-circulating tumor cells with the brain endothelium.

In our model, highly metastatic breast adenocarcinoma cells were used. Single cell force spectroscopy was applied to measure the de-

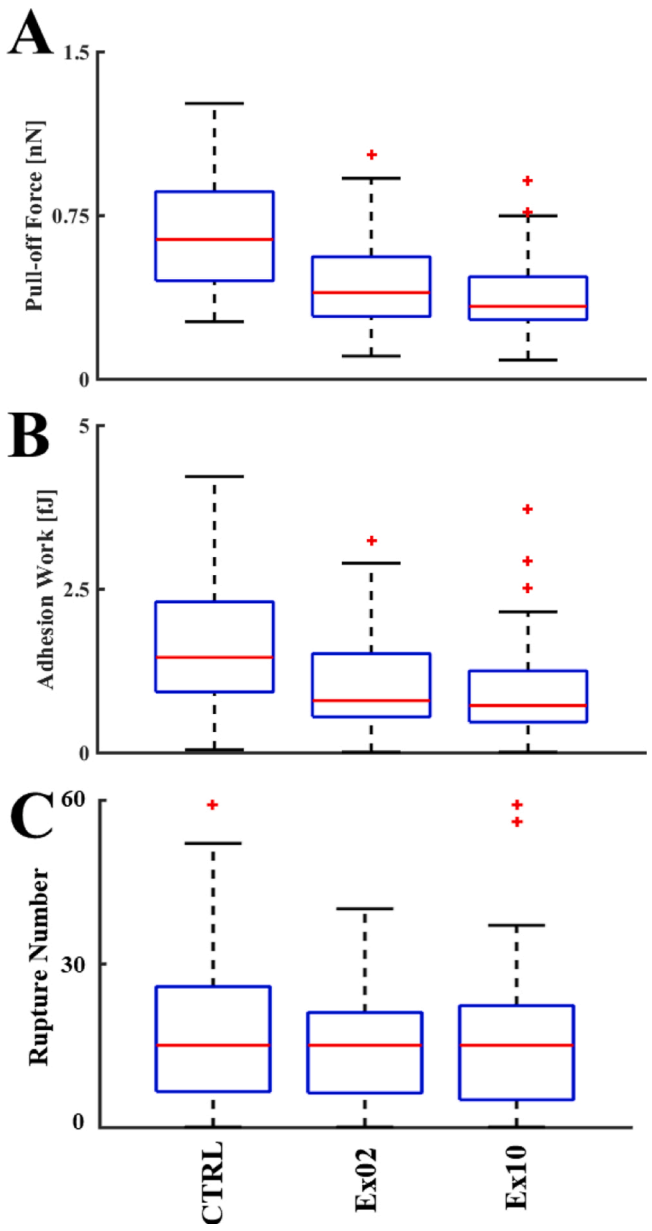

Fig. 4. Representative comparison of de-adhesion force (panel A), adhesion work (panel B) and number of ruptures (panel C) as measured between tumor cell and endothelial cells pre-treated for 24 h with exosomes. The three groups were the non-treated (CTRL) cells, the endothelial layer pre-treated with 2.5 μg/mL (Ex02) and 10 μg/mL (Ex10) of exosomes. Outliers are marked with red plus signs. Values out of +/- 2.7-fold the third quartile were regarded as outliers.

adhesion pattern of tumor cells from brain endothelium [23].

Pre-treatment with exosomes for 24 h was applied [25,28], in order to model processes that might occur after the cargo or exosome bodies themselves are taken up by the endothelial cells. Fig. 3 presents the uptake and localization of exosomes within endothelial cells after 24 h of treatment. For de-adhesion measurements the exosomes were administered in four different concentrations, at each experiment having pairs of 2.5 with 10, and 5 with 20 μg/mL. Here we have to mention, that these concentrations refer to the protein content of the exosome solution.

It has been shown, that MDA-MB-231 cells derived exosomes contain elevated level of EpCAM molecules [29]. This might point towards an elevated adhesiveness of the exosomes, however when they are incorporated into host cells, direct effect might be hindered by several factors.

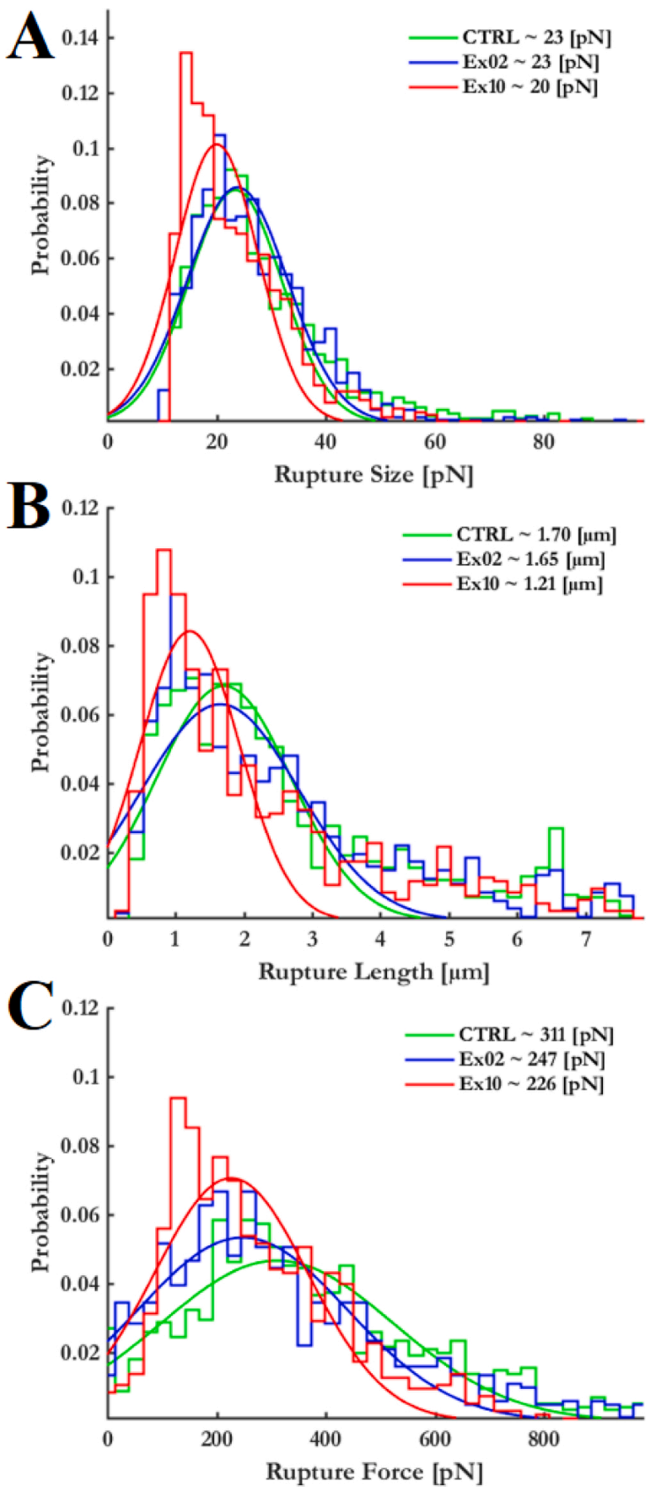

Fig. 5. Rupture Size (Panel A), rupture length (panel B) and rupture force (panel C) distribution extracted from the curves recorded. Presented values mark the most frequent value (maximum of fitted bell curves).

Our results indicate, that presence of exosomes lowers the adhesiveness of the endothelium when facing direct contact with breast adenocarcinoma cells. Size distribution of observed individual ruptures is close to those observed in case of cadherins [30,31] and membrane related connections, nanotube tethers [32]. The probability of occurrence shows a shift towards lower values (panel A of Fig. 5), as their occurring distance is closer to contact point (panel B of Fig. 5) in case of exosome treatment. Furthermore, they occur at lower force regimes

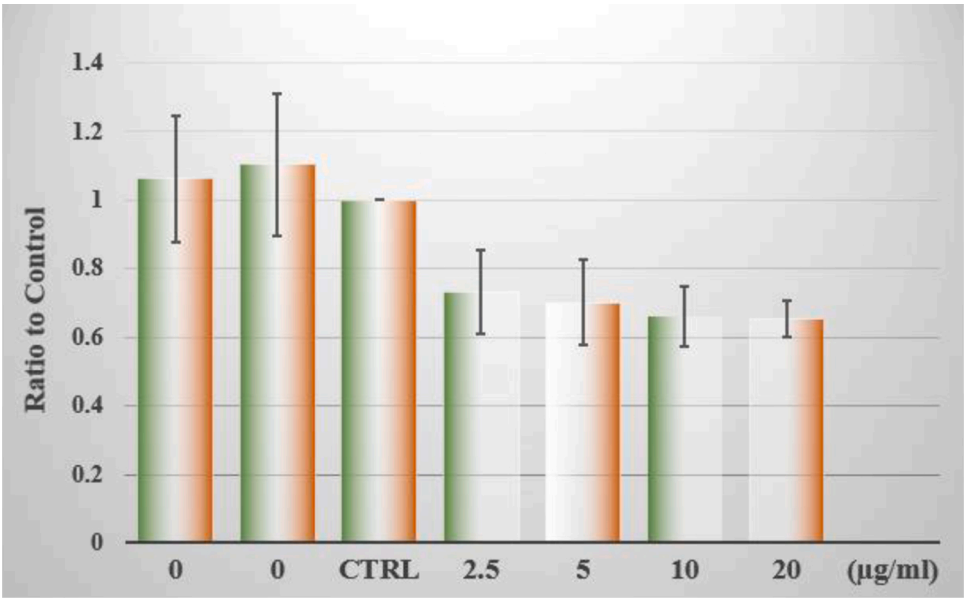

Fig. 6. Ratio of the measured de-adhesion forces as compared to control in function of the amount of exosomes. Groups were labelled by the concentration of exosomes in μg/mL they have received (0 equals CTRL case). Data is represented as mean ± standard deviation.

(panel C of Fig. 5), which means the established linkages are breaking up easier and quicker.

Cadherins may play important role in metastatic processes, their expression influences cellular adhesion in early stages [33]. The studied carcinoma cells lack while endothelial cell express N-cadherins [34]. Exosomes released by MDA-MB-231 cells might imbalance expression of cadherins in endothelial cells resulting in lower affinity to carcinoma cells in direct contact.

The other important factor in cell adhesiveness is the outer layer of glycoproteins. Their charge and density might influence and in certain circumstances hinder cell adhesion molecule related linkages. The presented direct measurement of de-adhesion parameters proves that presence of exosomes has effect on intercellular linkage. Although it may be transient, important consequences may arise. As shown in Fig. 3 there is enough time for endothelial cells to take up or fuse with the exosomes. The shift towards lower values of rupture size and rupture length (which is important parameter of invasiveness [23]) may indicate that formation and rupture of membrane nanotubes play important role in the established quick intercellular linkage.

Taken together, in the present study successful experimental setup was established in order to model the first contact of blood-circulating tumor cell with the brain endothelium. This first contact appeared to be weaker in case when endothelial cells were pre-treated with tumor cell derived exosomes. These results underline that first contact of blood circulating tumor cells might not be decisive in the process of metastasis formation, although pre-metastatic niches might play important role in final colonization.

Due to the complexity of the studied process, precise description points beyond the limit of the present study. These investigations might contribute to better understanding of what might be the crucial steps during brain metastasis progression.

CRediT authorship contribution statement

Csilla Fazakas: Conceptualization, Methodology, Visualization, Investigation, Data curation, Resources, Writing - review & editing. **Mihály Kozma:** Investigation, Data curation, Resources, Writing - review & editing. **Kinga Molnár:** Investigation, Data curation, Resources, Writing - review & editing. **András Kincses:** Investigation, Data curation, Resources, Writing - review & editing. **András Dér:** Supervision, Funding acquisition, Writing - review & editing. **Adrienn Fejér:** Investigation, Data curation, Resources, Writing - review & editing. **Barnabás Horváth:** Investigation, Data curation, Resources, Writing - review & editing. **Imola Wilhelm:** Supervision, Funding acquisition, Writing - review & editing. **István A. Krizbai:** Supervision, Funding acquisition, Writing - review & editing. **Attila G. Végh:** Conceptualization, Methodology, Visualization, Investigation, Data curation, Resources, Supervision, Funding acquisition, Software, Project administration, Validation, Writing - review & editing.

Declaration of Competing Interest

The authors report no declarations of interest.

Acknowledgements

This work was supported by the National Research, Development and Innovation Office of Hungary in the framework of the GINOP-2.3.2-15-2016-00037, GINOP-2.3.2-15-2016-00020 programs, the National Science Fund of Hungary OTKA PD121130, FK128654, FK124114, K135425, K135475 and by the Romanian Ministry of Education and Research within the frame of PN-III-P1-1.1-TE-2019-1302, PN-III-P4-ID-PCE-2020-1529 (UEFISCDI) programs. Csilla Fazakas was supported by the Janos Bolyai fellowship (BO/00213/19/8) of the Hungarian Academy of Sciences. Kinga Molnár was supported by New National Excellence Program of the Ministry for Innovation and Technology of Hungary (ÚNKP-20-4-SZTE-138).

References

[1] J. Gállego Pérez-Larraya, J. Hildebrand, Brain metastases, Handb. Clin. Neurol. 121 (2014) 1143–1157, https://doi.org/10.1016/B978-0-7020-4088-7.00077-8.
[2] R. Soffietti, P. Cornu, J.Y. Delattre, R. Grant, F. Graus, W. Grisold, J. Heimans, J. Hildebrand, P. Hoskin, M. Kalljo, P. Krauseneck, C. Marosi, T. Siegal, C. Vecht, EFNS guidelines on diagnosis and treatment of brain metastases: report of an EFNS task force, Eur. J. Neurol. 13 (2006) 674–681, https://doi.org/10.1111/j.1468-1331.2006.01506.x.
[3] I. Wortzel, S. Dror, C.M. Kenific, D. Lyden, Exosome-mediated metastasis: communication from a distance, Dev. Cell 49 (2019) 347–360, https://doi.org/10.1016/j.devcel.2019.04.011.
[4] T.B. Steinbichler, J. Dudás, H. Riechelmann, I.-I. Skvortsova, The role of exosomes in cancer metastasis, Semin. Cancer Biol. 44 (2017) 170–181, https://doi.org/10.1016/j.semcancer.2017.02.006.

[5] J. Dai, Y. Su, S. Zhong, L. Cong, B. Liu, J. Yang, Y. Tao, Z. He, C. Chen, Y. Jiang, Exosomes: key players in cancer and potential therapeutic strategy, Signal Transduct. Target. Ther. 5 (2020) 1–10, https://doi.org/10.1038/s41392-020-00261-0.
[6] T. Ando, Atomic force microscope: application to life science, Seikagaku 74 (2002) 1329–1342.
[7] M. Li, N. Xi, Y. Wang, L. Liu, Atomic force microscopy for revealing micro/nanoscale mechanics in tumor metastasis: from single cells to microenvironmental cues, Acta Pharmacol. Sin. (2020) 1–17, https://doi.org/10.1038/s41401-020-0494-3.
[8] S. Sharma, B.M. Gillespie, V. Palanisamy, J.K. Gimzewski, Quantitative nanostructural and single-molecule force spectroscopy biomolecular analysis of human-saliva-derived exosomes, Langmuir ACS J. Surf. Colloids 27 (2011) 14394–14400, https://doi.org/10.1021/la2038763.
[9] S. Sharma, M. Leclaire, J.K. Gimzewski, Ascent of atomic force microscopy as a nanoanalytical tool for exosomes and other extracellular vesicles, Nanotechnology (2018), https://doi.org/10.1088/1361-6528/aaab06.
[10] A. Hoshino, B. Costa-Silva, T.-L. Shen, G. Rodrigues, A. Hashimoto, M. Tesic Mark, H. Molina, S. Kohsaka, A. Di Giannatale, S. Ceder, S. Singh, C. Williams, N. Soplop, K. Uryu, L. Pharmer, T. King, L. Bojmar, A.E. Davies, Y. Ararso, T. Zhang, H. Zhang, J. Hernandez, J.M. Weiss, V.D. Dumont-Cole, K. Kramer, L.H. Wexler, A. Narendran, G.K. Schwartz, J.H. Healey, P. Sandstrom, K.J. Labori, E.H. Kure, P. M. Grandgenett, M.A. Hollingsworth, M. de Sousa, S. Kaur, M. Jain, K. Mallya, S. K. Batra, W.R. Jarnagin, M.S. Brady, O. Fodstad, V. Muller, K. Pantel, A.J. Minn, M. J. Bissell, B.A. Garcia, Y. Kang, V.K. Rajasekhar, C.M. Ghajar, I. Matei, H. Peinado, J. Bromberg, D. Lyden, Tumour exosome integrins determine organotropic metastasis, Nature 527 (2015) 329–335, https://doi.org/10.1038/nature15756.
[11] T. Ju, S. Wang, J. Wang, F. Yang, Z. Song, H. Xu, Y. Chen, J. Zhang, Z. Wang, A study on the effects of tumor-derived exosomes on hepatoma cells and hepatocytes by atomic force microscopy, Anal. Methods Adv. Methods Appl. (2020), https://doi.org/10.1039/d0ay01730b.
[12] M. Stec, R. Szatanek, M. Baj-Krzyworzeka, J. Baran, M. Zembala, J. Barbasz, A. Waligórska, J.W. Dobrucki, B. Mytar, A. Szczepanik, M. Siedlar, G. Drabik, B. Urbanowicz, M. Zembala, Interactions of tumour-derived micro(nano)vesicles with human gastric cancer cells, J. Transl. Med. 13 (2015) 376, https://doi.org/10.1186/s12967-015-0737-0.
[13] B. Whitehead, L. Wu, M.L. Hvam, H. Aslan, M. Dong, L. Dyrskjøt, M.S. Ostenfeld, S. M. Moghimi, K.A. Howard, Tumour exosomes display differential mechanical and complement activation properties dependent on malignant state: implications in endothelial leakiness, J. Extracell. Vesicles 4 (2015) 29685, https://doi.org/10.3402/jev.v4.29685.
[14] E.S. Grigoryeva, O.E. Savelieva, N.O. Popova, N.V. Cherdyntseva, V.M. Perelmuter, Do tumor exosome integrins alone determine organotropic metastasis? Mol. Biol. Rep. 47 (2020) 8145–8157, https://doi.org/10.1007/s11033-020-05826-4.
[15] R.J. Lobb, L.G. Lima, A. Möller, Exosomes: key mediators of metastasis and pre-metastatic niche formation, Semin. Cell Dev. Biol. 67 (2017) 3–10, https://doi.org/10.1016/j.semcdb.2017.01.004.
[16] Y. Guo, X. Ji, J. Liu, D. Fan, Q. Zhou, C. Chen, W. Wang, G. Wang, H. Wang, W. Yuan, Z. Ji, Z. Sun, Effects of exosomes on pre-metastatic niche formation in tumors, Mol. Cancer 18 (2019) 39, https://doi.org/10.1186/s12943-019-0995-1.
[17] B.B. Weksler, E.A. Subileau, N. Perrière, P. Charneau, K. Holloway, M. Leveque, H. Tricoire-Leignel, A. Nicotra, S. Bourdoulous, P. Turowski, D.K. Male, F. Roux, J. Greenwood, I.A. Romero, P.O. Couraud, Blood-brain barrier-specific properties of a human adult brain endothelial cell line, FASEB J. Off. Publ. Fed. Am. Soc. Exp. Biol. 19 (2005) 1872–1874, https://doi.org/10.1096/fj.04-3458fje.
[18] A.R. Bizzarri, A.G. Végh, G. Váró, S. Cannistraro, Interaction force fluctuations in antigen–antibody biorecognition studied by atomic force spectroscopy, ACS Omega 4 (2019) 3627–3634, https://doi.org/10.1021/acsomega.8b02993.
[19] J.L. Hutter, J. Bechhoefer, Calibration of atomic-force microscope tips, Rev. Sci. Instrum. 64 (1993) 1868–1873, https://doi.org/10.1063/1.1143970.
[20] R. Proksch, T.E. Schaffer, J.P. Cleveland, R.C. Callahan, M.B. Viani, Finite optical spot size and position corrections in thermal spring constant calibration, Nanotechnology 15 (2004) 1344–1350.
[21] J.E. Sader, J.W.M. Chon, P. Mulvaney, Calibration of rectangular atomic force microscope cantilevers, Rev. Sci. Instrum. 70 (1999) 3967–3969, https://doi.org/10.1063/1.1150021.
[22] M.J. Higgins, M. Polcik, T. Fukuma, J.E. Sader, Y. Nakayama, S.P. Jarvis, Structured water layers adjacent to biological membranes, Biophys. J. 91 (2006) 2532–2542, https://doi.org/10.1529/biophysj.106.085688.
[23] B. Varga, R.A. Domokos, C. Fazakas, I. Wilhelm, I.A. Krizbai, Z. Szegletes, C. Gergely, G. Váró, A.G. Végh, De-adhesion dynamics of melanoma cells from brain endothelial layer, Biochim. Biophys. Acta BBA - Gen. Subj. 1862 (2018) 745–751, https://doi.org/10.1016/j.bbagen.2017.10.013.
[24] A.G. Végh, C. Fazakas, K. Nagy, I. Wilhelm, J. Molnár, I.A. Krizbai, Z. Szegletes, G. Váró, Adhesion and stress relaxation forces between melanoma and cerebral endothelial cells, Eur. Biophys. J. 41 (2012) 139–145, https://doi.org/10.1007/s00249-011-0765-5.
[25] G. Rodrigues, A. Hoshino, C.M. Kenific, I.R. Matei, L. Steiner, D. Freitas, H.S. Kim, P.R. Oxley, I. Scandariato, I. Casanova-Salas, J. Dai, C.R. Badwe, B. Gril, M. Tešić Mark, B.D. Dill, H. Molina, H. Zhang, A. Benito-Martin, L. Bojmar, Y. Ararso, K. Offer, Q. LaPlant, W. Buehring, H. Wang, X. Jiang, T.M. Lu, Y. Liu, J.K. Sabari, S. J. Shin, N. Narula, P.S. Ginter, V.K. Rajasekhar, J.H. Healey, E. Meylan, B. Costa-Silva, S.E. Wang, S. Rafii, N.K. Altorki, C.M. Rudin, D.R. Jones, P.S. Steeg, H. Peinado, C.M. Ghajar, J. Bromberg, M. de Sousa, D. Pisapia, D. Lyden, Tumour exosomal CEMIP protein promotes cancer cell colonization in brain metastasis, Nat. Cell Biol. 21 (2019) 1403–1412, https://doi.org/10.1038/s41556-019-0404-4.
[26] K.E. Malek-Zietek, M. Targosz-Korecka, M. Szymonski, The impact of hyperglycemia on adhesion between endothelial and cancer cells revealed by single-cell force spectroscopy, J. Mol. Recognit. JMR. 30 (2017) e2628, https://doi.org/10.1002/jmr.2628.
[27] S. Azadi, M. Tafazzoli-Shadpour, R. Omidvar, L. Moradi, M. Habibi-Anbouhi, Epidermal growth factor receptor targeting alters gene expression and restores the adhesion function of cancerous cells as measured by single cell force spectroscopy, Mol. Cell. Biochem. 423 (2016) 129–139, https://doi.org/10.1007/s11010-016-2831-x.
[28] A. Hoshino, B. Costa-Silva, T.-L. Shen, G. Rodrigues, A. Hashimoto, M.T. Mark, H. Molina, S. Kohsaka, A.D. Giannatale, S. Ceder, S. Singh, C. Williams, N. Soplop, K. Uryu, L. Pharmer, T. King, L. Bojmar, A.E. Davies, Y. Ararso, T. Zhang, H. Zhang, J. Hernandez, J.M. Weiss, V.D. Dumont-Cole, K. Kramer, L.H. Wexler, A. Narendran, G.K. Schwartz, J.H. Healey, P. Sandstrom, K.J. Labori, E.H. Kure, P. M. Grandgenett, M.A. Hollingsworth, M. de Sousa, S. Kaur, M. Jain, K. Mallya, S. K. Batra, W.R. Jarnagin, M.S. Brady, O. Fodstad, V. Muller, K. Pantel, A.J. Minn, M. J. Bissell, B.A. Garcia, Y. Kang, V.K. Rajasekhar, C.M. Ghajar, I. Matei, H. Peinado, J. Bromberg, D. Lyden, Tumour exosome integrins determine organotropic metastasis, Nature 527 (2015) 329, https://doi.org/10.1038/nature15756.
[29] S. Kruger, Z.Y.A. Elmageed, D.H. Hawke, P.M. Wörner, D.A. Jansen, A.B. Abdel-Mageed, E.U. Alt, R. Izadpanah, Molecular characterization of exosome-like vesicles from breast cancer cells, BMC Cancer 14 (2014) 44, https://doi.org/10.1186/1471-2407-14-44.
[30] P. Panorchan, M.S. Thompson, K.J. Davis, Y. Tseng, K. Konstantopoulos, D. Wirtz, Single-molecule analysis of cadherin-mediated cell-cell adhesion, J. Cell. Sci. 119 (2006) 66–74, https://doi.org/10.1242/jcs.02719.
[31] L.A. Chtcheglova, J. Waschke, L. Wildling, D. Drenckhahn, P. Hinterdorfer, Nano-scale dynamic recognition imaging on vascular endothelial cells, Biophys. J. 93 (2007) L11–13, https://doi.org/10.1529/biophysj.107.109751.
[32] M. Sun, J.S. Graham, B. Hegedus, F. Marga, Y. Zhang, G. Forgacs, M. Grandbois, Multiple membrane tethers probed by atomic force microscopy, Biophys. J. 89 (2005) 4320–4329, https://doi.org/S0006-3495(05)73072-1 [pii].
[33] R. Omidvar, M. Tafazzoli-Shadpour, M.A. Shokrgozar, M. Rostami, Atomic force microscope-based single cell force spectroscopy of breast cancer cell lines: an approach for evaluating cellular invasion, J. Biomech. 47 (2014) 3373–3379, https://doi.org/10.1016/j.jbiomech.2014.08.002.
[34] H. Herman, C. Fazakas, J. Haskó, K. Molnár, Á. Mészáros, Á. Nyúl-Tóth, G. Szabó, F. Erdélyi, A. Ardelean, A. Hermenean, I.A. Krizbai, I. Wilhelm, Paracellular and transcellular migration of metastatic cells through the cerebral endothelium, J. Cell. Mol. Med. 23 (2019) 2619–2631, https://doi.org/10.1111/jcmm.14156.